Journal of
Composites Science

MDPI

Article

Composite Materials Based on Spent Coffee Grounds and Paper Pulp

Victoria Bejenari [1], Maricel Danu [1,2,*], Alina-Mirela Ipate [2], Mirela-Fernanda Zaltariov [2], Daniela Rusu [2] and Gabriela Lisa [1,*]

[1] Faculty of Chemical Engineering and Environmental Protection "Cristofor Simionescu", Gheorghe Asachi Technical University of Iasi, 73 Prof. dr. doc D. Mangeron Street, 700050 Iasi, Romania; victoria.bejenari@tuiasi.ro
[2] Petru Poni Institute of Macromolecular Chemistry, 41A Aleea Gr. Ghica Voda, 700487 Iasi, Romania; ipate.alina@icmpp.ro (A.-M.I.); zaltariov.mirela@icmpp.ro (M.-F.Z.); rusu.daniela@icmpp.ro (D.R.)
* Correspondence: maricel.danu@academic.tuiasi.ro (M.D.); gabriela.lisa@academic.tuiasi.ro (G.L.)

Abstract: The need for biodegradable and environmentally friendly materials is increasing due to resource shortages and rising levels of environmental pollution. Agro-food waste, which includes coffee grounds, is of great interest in the production of composite materials due to its low cost, low density, easy availability, non-abrasive nature, specific properties such as reduced wear on the machinery used, the absence of residues and toxic products, and biodegradable characteristics. The composite materials developed that include coffee grounds exhibit good characteristics. This field is evolving and requires further improvements, but, at this moment, it can be stated that coffee grounds are not just waste but can be transformed into a highly efficient material applicable in various domains. In this study, composite materials were prepared using paper pulp as a matrix, coffee grounds as a filler material, and water as a binding agent. The obtained composite materials were evaluated through thermal analysis, SEM, EDX, ATR-FTIR, and rheological behavior analysis. The composite materials created from paper pulp and coffee grounds proved to be effective for use in the production of seedling pots. The seedling pots created in this study are produced at a low cost, are environmentally friendly, exhibit thermal stability, have good stability over time, and have good resistance to deformation.

Keywords: spent coffee grounds; paper pulp; composite materials; seedling pots; sustainability; environmentally friendly materials

check for updates

Citation: Bejenari, V.; Danu, M.; Ipate, A.-M.; Zaltariov, M.-F.; Rusu, D.; Lisa, G. Composite Materials Based on Spent Coffee Grounds and Paper Pulp. *J. Compos. Sci.* **2024**, *8*, 491. https://doi.org/10.3390/jcs8120491

Academic Editor: Vincenzo Fiore

Received: 21 October 2024
Revised: 19 November 2024
Accepted: 22 November 2024
Published: 24 November 2024

Copyright: © 2024 by the authors. Licensee MDPI, Basel, Switzerland. This article is an open access article distributed under the terms and conditions of the Creative Commons Attribution (CC BY) license (https://creativecommons.org/licenses/by/4.0/).

1. Introduction

The International Coffee Organization (ICO) estimated the global coffee consumption to reach 177 million 60 kg bags in 2023/2024 [1]. In 2022/2023, approximatively 3 billion cups of coffee were consumed daily worldwide. From this sector, around 11.14 million tons of spent coffee grounds (61% moisture content) were generated, which corresponds to approximately 6.92 million tons of dry material [2]. During coffee preparation, only 0.2 wt% of the coffee bean is subjected to the extraction, while the rest results as coffee waste, specifically spent coffee grounds (SCGs) [3]. SCGs can be considered to be a value-added product due to their important and rich physicochemical composition, which includes (*w*/*w*) 30–40% hemicellulose, 8.6–13.3% cellulose, 25–33% lignin, around 2.5%polyphenols, as well as various polysaccharides, fatty acids, minerals, and other compounds [4,5].

Considering the valuable composition of SCGs, the principle of green chemistry, and the significance of a circular bio-economy for a sustainable environment, numerous applications for SCGs have been proposed and investigated. The main directions for their applicability include the production of bio-syngas [6,7], electricity [8], biodiesel [9–13], compost [14], bio-sorbent for bioremediation processes [15–21], production of biochar [13,22–29],

hydrochar [30–34], activated carbon [21,35–39], and the design of biocomposite materials [40–44]. Additionally, SCGs serve as a valuable raw material for the production of enzymes [5,45], bioethanol [7,46,47], polyhydroxyalkanoate polymers [48], and biogas [49–55].

In recent years, there has been a particular interest in the integrated valorization of SCGs for developing "green" and sustainable composites. SCGs have been used as filler in the design of thermoset materials to improve the physical, mechanical, thermal, and structural properties. This approach also aims to reduce the production costs of composites, minimize waste generation, and enhance the biodegradability of the materials [41,43,56]. SCGs have been used as filler in different types of polymer matrixes: polypropylene, polyethylene, polyurethane, poly(lactic acid), Poly(Butylene Adipate-Co-Terephthalate), polyvinyl alcohol (PVA), epoxy resins, rubber, and others [57]. Alharbi et al. demonstrated that the addition of grounds SCGs as a microfiller in poly-3-hydro-xybutyrate-co-3-hydroxyvalerate (PHBV) biopolymer enhanced the overall mechanical properties and improved the structural characteristics of the biocomposites [58]. Moustafa et al. used biodegradable SCGs as a filler in a poly(butylene adipate-co-terephthalate) (PBAT) matrix to create green composites at an affordable cost [59]. Cataldo et al. developed a novel composite bioplastic based on a pectin matrix and SCGs as a filler. Improvements in the mechanical properties of the biocomposites were reported [60]. Nanocomposites were designed by Lee et al. in which CGs were dispersed in a polyvinyl alcohol (PVA) matrix. The nanocomposites exhibited significantly improved mechanical properties, such as tensile strength and Young's modulus [61]. In order to reduce the production costs of biocomposites, Masssijaya et al. [44] added SCGs to polylactic acid (PLA) and thermoplastic starch (TPS). Additionally, de Bomfim et al. [62] reported increases in crystallinity and viscoelastic behavior when SCGs were incorporated into PLA. These composites have potential applications as replacements for conventional PLA products (packaging or 3D printing). Nguyen et al. [56] designed an environmentally friendly epoxy composite in the presence of lime-treated SCGs. To reduce waste generation, Jaramillo et al. [63] proposed to use coffee husk as a filler and polyethylene as the matrix in projecting eco-composites. As observed, most studies report the use of SCGs as filler in polymer matrices. However, a major focus in the development of green and sustainable composites is the replacement of the polymeric matrix with a natural matrix derived from biomass. Additionally, these studies focus on designing biodegradable composites or reducing plastic use, while a major area of interest in the composite sector is designing them with concepts such as bio-based materials, full recyclability, or even compostability, in contrast to the conventional synthetic composites.

Approximately 17 wt% of the global waste comes from the paper industry, with around 186 thousand tons generated from the pulp and paper industry [64]. Due to its high availability, pulp paper can be considered to be a valuable matrix in composite materials. Pulp paper has been used in the development of food packaging [65,66], e.g., egg containers, beverage cups, for planting pots [67], packaging of electronics [68], and others. The main advantages of paper pulp are its renewable character, which make it an environmentally friendly material, along with its cost-effectiveness [69,70].

The innovative aspect of this study is the combination of paper pulp with SCGs. The main goals of this work are the following: (i) to prepare green and environmentally friendly composite materials using paper pulp as a matrix, SCGs as a filler material, and water as a binding agent; (ii) to evaluate the effect of SCG content variation on the physical, structural, and thermal properties, as well as rheological behavior of the composite materials; and (iii) to demonstrate the use of SCGs as a filler in composite materials in order to generate seedling pots. Furthermore, the study focuses on the effectiveness of valorizing these two waste-derived components (paper pulp and CGs) into cost-effective and eco-friendly composite materials. To the best of our knowledge, none of these aspects have been previously investigated.

2. Materials and Methods

2.1. Method for Producing Composite Materials

Biodegradable polymers are still very expensive and not economically competitive compared to basic plastics. An analysis of the future prospects of the global and European biodegradable plastics market was recently conducted by Döhler et al. [71]. The results indicate significant growth potential in the coming years, with an average annual growth rate of 4.98% for global production, although this may be sensitive to the impacts of economic and political factors. The properties and costs of biodegradable polymers can be modified and improved by using lignocellulosic fibers, which can reduce the cost of a material without affecting its biodegradability. Natural fibers are considered to be suitable materials for composites because they can combine good mechanical properties with ecological advantages due to their abundance and biodegradability [72]. Based on these characteristics of natural fibers, a composite material is proposed using paper pulp as the matrix, SCGs as the filler material, and water as the binding agent (Figure 1). Water facilitates the mixing and rehydration of the cellulosic fibers in the paper pulp, allowing them to connect through networks of weak bonds (hydrogen bonds) [73]. Upon evaporation of the water, the composite becomes more rigid. Cellulose fibers ensure the cohesion of the composite and the uniform distribution of filler particles, specifically SCGs, which contribute to increasing the rigidity of the material.

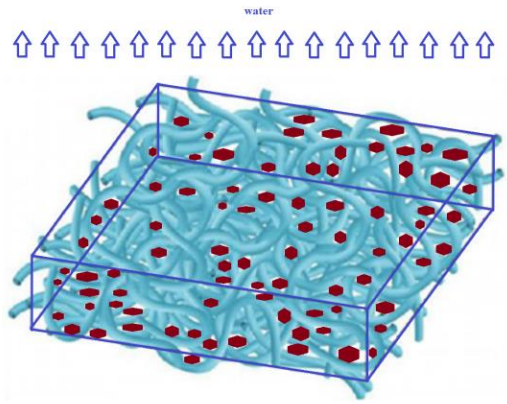


Figure 1. Schematic representation of the structure of the composite material.

Various types of coffee are available commercially, most of which contain different blends of Arabica and Robusta coffee. From this perspective, this study focuses on SCGs from GB coffee, which contains 50% Arabica coffee and 50% Robusta coffee.

Following a physicochemical characterization study of six types of SCGs, this one proved to be the most suitable, with better contents of minerals and macronutrients (Ca, K, Mg, Na, S, and P) and lower contents of C, O, and N compared to the other samples [74].

To obtain the composite material, the mass ratio of ingredients and the preparation method of the samples were varied. For sample preparation, different amounts of SCGs and paper pulp were added to a stainless steel plate. Each sample was prepared at room temperature, with no pressure applied, by manually blending SCGs with paper pulp to obtain a homogeneous mixture. Subsequently, water was gradually added to the SCG–paper pulp blend with continuous manual mixing until a paste-like consistency was formed. The mixtures were then transferred into a silicone mold and dried in a tray dryer at 70 °C until constant mass was achieved. It was found that the best results were obtained when warm water was used, added in the final stage, and a ratio of paper pulp/water 1:1 was applied.

Since SCGs have a high water absorption capacity (3.7701 $\pm$ 0.2 g of dry grounds per g of water) [75], the necessity of using an excess amount of water was observed to achieve better bonding of the sample.

Before being used for composite material production, SCGs were dried for 4 h in a tray dryer at a temperature of approximately 70 °C. These parameters were used to achieve a humidity of approximately 5%, established using the Mettler Toledo HG63 Halogen Humidity Analyzer.

To obtain the optimal composition, seven samples with different concentrations of SCGs were analyzed, as presented in Table 1. The SCG percentage was considered as the independent variable in the experimental planning. This ranged between 40% and 65%, with a variation interval regarding the independent variable of ±5%. The amounts of paper pulp and water were considered to be equal to half the remaining percentage up to 100%, with a variation interval of ±2.5%.

Table 1. Percent compositions of analyzed samples.

Sample	Sample Image	Ingredients, %		
		Spent Coffee Grounds	Paper Pulp	Water
1		-	50	50
2		40	30	30
3		45	27.5	27.5
4		50	25	25
5		55	22.5	22.5
6		60	20	20
7		65	17.5	17.5

2.2. Techniques for Characterizing Composite Materials

Thermal analysis of the samples was carried out by recording thermogravimetric (TG), derivative thermogravimetric (DTG), and differential thermal (DTA) curves using a Mettler 851^e derivatograph. The tests were performed under dynamic conditions, with nitrogen at a flow rate of 20 mL/min, a heating rate of 10 °C/min, and within a temperature

range of 25–700 °C. The sample masses varied between 3.39 and 4.73 mg. The very good sensitivity of the equipment used enabled the use of small sample quantities, which have the advantage of uniform heat transfer, thus reducing temperature gradients within the sample. Additionally, the samples were very well homogenized, and multiple tests were performed under the same conditions for each composite.

The surface morphology of the unmetallized samples mounted on aluminum stubs by double-band carbon tape was examined by using a Scanning Electron Microscope (SEM) type Quanta 200 (FEI, Eindhoven, Netherlands) operating at 20 kV with secondary electrons in low vacuum mode using LFD (Large Field Detector, Thermo Fisher Scientific, Eindhoven, Netherlands). SEM micrographs were recorded at different magnifications for each sample. Afterwards, the same samples used for SEM measurements were submitted to EDX analysis. The Quanta 200 microscope is equipped with an energy-dispersive X-ray system (EDX) for qualitative analysis and elemental mapping. The EDX detector used is the silicon-drift detector, which enables rapid determination of elemental compositions and acquisition of compositional maps. All the samples are imaged at 10 mm WD (working distance), which is the stage eucentric position and the collection point of the EDX detector. It is used in conjunction with the LFD detector.

FTIR spectra were recorded using a Bruker Vertex 70 FTIR spectrometer (Bruker Optics, Ettlingen, Germany) with standard configuration: Mid-IR (MIR) source that enables the identification of common functional groups and bonds for organic molecules, KBr beamsplitter, and DLaTGS detector. The spectra were registered in Attenuated Total Reflectance (ATR) using an ATR Pike MIRacle device equipped with a ZnSe crystal. ZnSe crystal enables the spectra measurements in the range 600–4000 cm^{-1}. In ATR technique, the samples are analyzed in their native state without additional preparation or destruction stages. Measurements were carried out at room temperature with a resolution of 4 cm^{-1} and 32 scans. The spectra were processed in OPUS software, version 6.5 (suitable for acquisition of data, spectra processing, and analysis) following these steps: water and CO_2 compensations, ATR→absorbance (AB) conversion, baseline correction, and normalization.

The obtained composites were exposed to irradiation for the study of artificial aging, and the stability of the samples was estimated using the crystallinity index determined from IR spectra. A laser source with a wavelength of 355 nm and an irradiation frequency of 500 mm/s was used.

The rheological behavior of the obtained composite materials was studied with a Physica MCR 501 rheometer (Anton Paar, Graz, Austria) using a parallel plate measuring system with a diameter of 50 mm. Serrated plates were used to avoid material slippage between the plates. The samples were rheologically analyzed using two types of oscillatory tests: amplitude sweep and frequency sweep. The amplitude sweeps were performed in the strain domain 0.001–0.1%. The frequency sweeps were performed at a constant amplitude of 0.005% or 0.01% (in the LVE range characteristic for each sample) over a frequency range between 0.1 and 100 rad/s. Both rheological tests were performed at a constant temperature of 25 °C. The samples were conditioned in the form of discs with a diameter of approximately 50 mm and a thickness between 2.7 and 4 mm.

3. Results

3.1. Obtaining Composite Materials

The samples prepared according to the formulations in Table 1 were dried. After this process, weighing revealed that the water content in the samples had fully evaporated. Consequently, the proportions of SCGs and paper pulp were adjusted, as shown in Table 2. It is important to note that the experiment was conducted in triplicate for each sample type.

Table 2. The percentage compositions of the analyzed samples after drying.

Sample	Ingredients, %	
	Spent Coffee Grounds	Paper Pulp
1	-	100
2	57.02484 ± 0.016	42.97516 ± 0.016
3	62.20738 ± 0.063	37.79262 ± 0.063
4	66.68399 ± 0.101	33.31801 ± 0.098
5	71.05051 ± 0.141	28.94949 ± 0.141
6	74.88531 ± 0.087	25.11469 ± 0.087
7	78.7031 ± 0.132	21.2969 ± 0.132

The samples were poured in their wet state into silicone molds, and, once dried, they were transformed into seedling pots. Figure 2 presents several examples of pots created from composite materials 5, 6, and 7.



Figure 2. Seedling pots created from composite materials.

3.2. Characterization of the Obtained Composite Materials

3.2.1. Thermal Analysis (TG, DTG, and DTA)

Figure 3a,b show a comparative presentation of the TG and DTG curves for the seven samples subjected to thermogravimetric analysis. The thermogravimetric curves provide information regarding the thermal stability of the analyzed samples. The main thermogravimetric characteristics obtained from the curves are T_i—the temperature at which degradation begins; T_m—the temperature at which the degradation rate is at its maximum; T_f—the temperature at which the degradation process is completed; and W—the percentage of mass loss and the amount of residue, which are presented in Table 3.

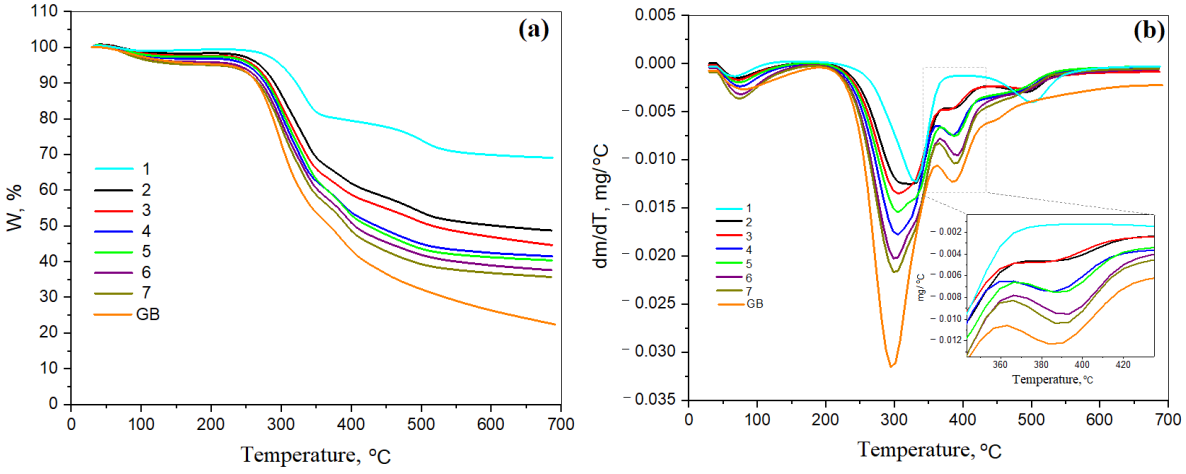


Figure 3. Thermogravimetric curves. (**a**) TG curves. (**b**) DTG curves.

Table 3. Thermogravimetric characteristics.

Sample	Stage 1				Stage 2				Stage 3				Stage 4				Residue
	T_i	T_m	T_f	W	T_i	T_m	T_f	W	T_i	T_m	T_f	W	T_i	T_m	T_f	W	
	(°C)	(°C)	(°C)	(%)	(°C)	(°C)	(°C)	(°C)	(°C)	(°C)	(°C)	(%)	(°C)	(°C)	(°C)	(%)	(%)
1	40	66	99	1.26	283	331	349	20.01	-	-	-	-	467	501	524	10.39	68.34
2	55	69	119	2.49	263	322	349	29.26	349	388	404	8.41	446	498	519	11.96	47.88
3	51	70	103	3.00	262	304	346	31.47	346	384	399	7.54	399	495	519	14.19	43.8
4	50	74	105	3.65	262	301	342	32.96	342	386	401	10.42	401	485	514	11.99	40.98
5	49	72	100	3.21	266	302	348	34.39	348	391	405	11.08	405	486	508	11.60	39.72
6	55	74	121	4.43	260	300	347	34.66	347	391	408	11.88	408	497	517	11.50	37.53
7	48	72	111	5.29	262	301	345	35.43	345	393	406	12.15	406	503	512	11.93	35.2
GB	47.1	78.2	147.6	4.54	267	297.0	335.2	42.29	369.3	386.9	407.1	14.59	407.1	450.8	-	16.73	21.85

Regarding thermal stability, sample 1, which consists entirely of paper pulp, exhibits three distinct stages. The first stage involves the removal of water, which is present at a concentration of 1.26%. The other two stages involve thermal decomposition processes. The initial thermal decomposition stage begins at 283 °C, a temperature close to the value of 275 °C reported by Lengowski and his team for cellulose pulp [76]. This stage is linked to cellulose breakdown. Studies in the literature identify the primary components of paper pulp from various wood types as cellulose (65–70% [77], 74.5–94.5% [78]), hemicellulose (2.4–10% [78]), and lignin (12–17.6% [77], 2.9–13.5% [78]). The second stage of decomposition starts at 467°C and is characteristic of lignin breakdown. For this sample, the residue obtained is 68.34%.

For the other samples, which contain SCGs in different percentages, the removal of water (dehydration stage) occurs in a proportion of 2.49 to 5.29%. The first thermal decomposition stage begins at a temperature of 260–266 °C, a temperature very close to the first degradation stage of the SCGs—266 °C. In this stage, the depolymerization and decomposition of polysaccharides, such as hemicellulose and cellulose, occur [79,80].

For the samples containing SCGs, it is observed that, between the two thermal decomposition stages present in the 100% paper pulp sample, a new degradation stage appears, marked in Figure 3b. This is characteristic of the thermal behavior of the used SCGs, where the temperature at which degradation begins is 342–349 °C for those samples containing SCGs and 369 °C for the SCGs themselves. This stage may be associated with the decomposition of the oil present in the SCGs. In the study conducted by Dang and Nguyen regarding the thermal behavior of SCGs, it is noted that the stage of oil degradation from SCGs is reported at temperatures of 350–400 °C [81].

The last decomposition stage begins at temperatures of 399–408 °C. In this stage, the decomposition of lignin occurs, a stage also present in the thermal behavior of SCGs, which begins at a temperature of 407 °C. Similar values were obtained by Fermoso and Mašek, who associated the temperature of 395 °C with the stage of lignin decomposition [82].

In Figure 3a, it can be observed that, as the SCG content in the sample increases, the decomposition process is more advanced, resulting in smaller amounts of residue from one sample to another. The thermogravimetric curves for the different analyzed mixtures exhibit an intermediate behavior between the paper pulp and SCGs, as expected. The thermal behavior of the composite tends more towards the paper pulp or SCGs depending on the mass proportion of the latter in the composite. A similar behavior was also reported by Moustafa and his collaborators in their attempt to obtain composite materials using SCGs and poly(butylene adipate-co-terephthalate) (PBAT) [59].

3.2.2. Morphological Characterization (SEM and EDX)

The composite materials produced were morphologically analyzed using scanning electron microscopy (SEM). Figure 4 presents the SEM images at a magnification of 1000×. The SEM image for the material containing only paper pulp in Figure 4a highlights the

presence of cellulose microfibers [83]. In the other composite materials, which contain mixtures in different proportions of paper pulp and SCGs, the presence of cellulose microfibers as well as SCGs is also observed. The SCGs are highlighted by the presence of zones with a "sponge-like" appearance. The specialized software Image J 1.53 enabled the determination of the size of these zones, which may correspond to SCG particles embedded in the composite materials. The average values of these are presented in Table 4. We found that they range between 490 and 840 µm.

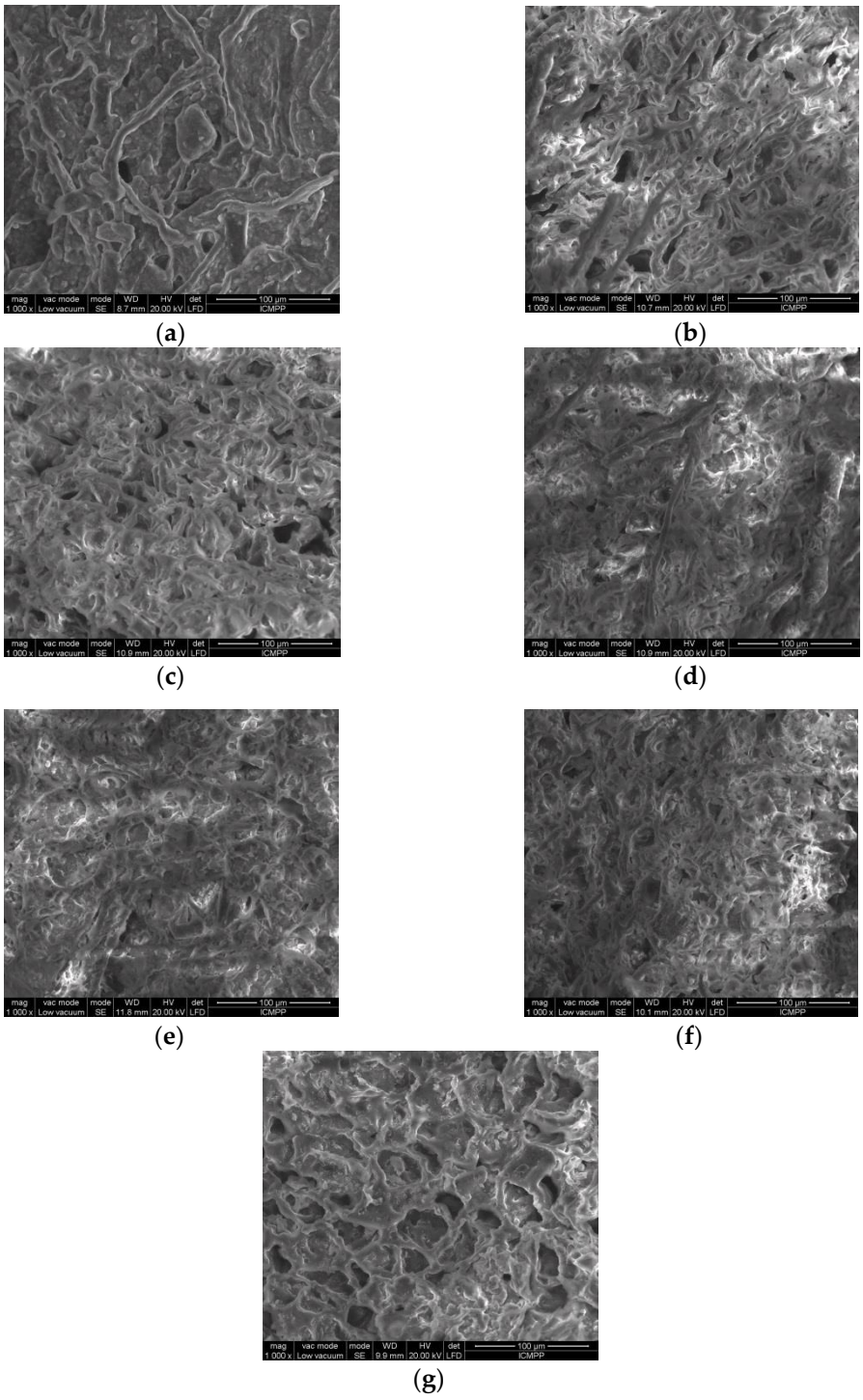


Figure 4. SEM images of the composite materials: 1 (**a**), 2 (**b**), 3 (**c**), 4 (**d**), 5 (**e**), 6 (**f**), and 7 (**g**) at 1000× magnification.

Table 4. Average sizes of SCG particles and macropores present in the composite materials.

Sample	2	3	4	5	6	7
$D_{average}$ (μm)	491.8 ± 47.9	542.1 ± 77.1	589.4 ± 19.8	657.5 ± 82.6	779.6 ± 19.5	836.8 ± 76.0
$d_{average}$ (μm)	20.4 ± 2.7	25.7 ± 3.7	13.9 ± 2.5	20.8 ± 3.3	20.0 ± 3.2	26.1 ± 3.7

The uniform presence of macropores is noted in samples 2, 3, 6, and 7. Using the specialized software Image J, their sizes were measured. The average values ($d_{average}$) obtained are presented in Table 4. In the case of composite materials 2, 5, and 6, the macropore sizes are around 20 μm; for 3 and 7, they are approximately 26 μm; and, for sample 4, around 14 μm. Pore sizes not exceeding 30 μm have also been reported for SCGs by other researchers [84,85].

In the case of composite materials 2, 3, 6, and 7, the presence of micropores with an average size of approximately 3 μm is also highlighted. Additionally, from the SEM images of sample 1, which contains only paper pulp, an average fiber diameter of approximately 12 μm was determined for the cellulose fibers. Hanafiah and others reported average cellulose fiber diameter values ranging between 6 and 16 μm for fibers extracted from recycled paper [86].

Given the targeted applications for the composite materials obtained in this study, specifically their use in the production of seedling pots, we believe that the presence of macro- and micropores may enable the absorption of moisture from the atmosphere and thus reduce the amount of water needed for plant growth.

Energy-dispersive X-ray spectroscopy was applied to the surfaces of the composite materials, allowing us to identify and characterize their elemental composition. Data were collected from three randomly selected points. The arithmetic mean of these values was considered, and the average weight percentage of the identified elements was calculated. The results are presented in Table 5. The same table also presents the previously obtained results for Granbar SCGs used in the production of composite materials [74].

Table 5. Average percentage compositions for composite materials and types of spent coffee grounds (GB).

	Elements, %							
	1	**2**	**3**	**4**	**5**	**6**	**7**	**GB**
C	27.70	45.64	48.72	44.95	56.31	49.27	51.25	65.39
N	1.51	2.49	2.69	2.45	2.52	2.96	1.71	4.56
O	45.47	37.05	35.27	37.91	31.71	35.74	34.77	28.79
Na	0.80	0.27	0.21	0.20	0.22	0.19	0.12	0.09
Mg	0.19	0.12	0.11	0.14	0.17	0.12	0.10	0.18
Al	11.19	6.10	5.71	6.19	3.58	5.08	5.15	-
Si	12.07	6.84	6.04	6.79	3.89	5.35	5.51	0.05
P	0.12	0.11	0.10	0.12	0.14	0.10	0.07	0.07
S	0.14	0.11	0.09	0.07	0.17	0.09	0.09	0.16
K	0.50	1.06	0.92	0.98	0.99	0.95	1.08	0.55
Ca	0.33	0.21	0.16	0.20	0.30	0.15	0.18	0.16

In the case of the material containing only paper pulp (1), we observed the lowest percentage of carbon (C), while the highest was found in the Granbar SCGs. For the composite materials created from SCGs and paper pulp, the percentage of carbon ranges from 44% to 56%. Another major element is oxygen (O), which has a percentage of approximately

29% for SCGs and 45% for paper pulp. Intermediate values ranging from 31% to 37% were determined for the composite materials. The material composed solely of paper pulp contains 11% to 12% aluminum (Al) and silicon (Si). These elements are also observed in the composite materials in percentages ranging from 3% to 7%.

The composite materials also contain nitrogen (N) in percentages ranging from 1.7% to 2.9%, potassium (K) at approximately 1%, and phosphorus (P) in percentages ranging from 0.07% to 0.12%. There are studies in the literature that confirm the potential use of SCGs or composite materials containing this waste from the food industry as fertilizers in agriculture [87–89].

The seedling pots produced in this study, which are obtained at a low cost and are eco-friendly, can be planted in the field along with the plants that have reached the appropriate development stage and can act as fertilizers. Additionally, due to their high porosity, they can help to maintain soil moisture and provide an opportunity to save water for irrigation.

3.2.3. Characterization by ATR-FTIR Spectrometry

The ATR-FTIR spectra for the six composite materials (2, 3, 4, 5, 6, and 7) are compared in Figure 5 with the spectra obtained for the Granbar SCGs and the material created exclusively from paper pulp (1).

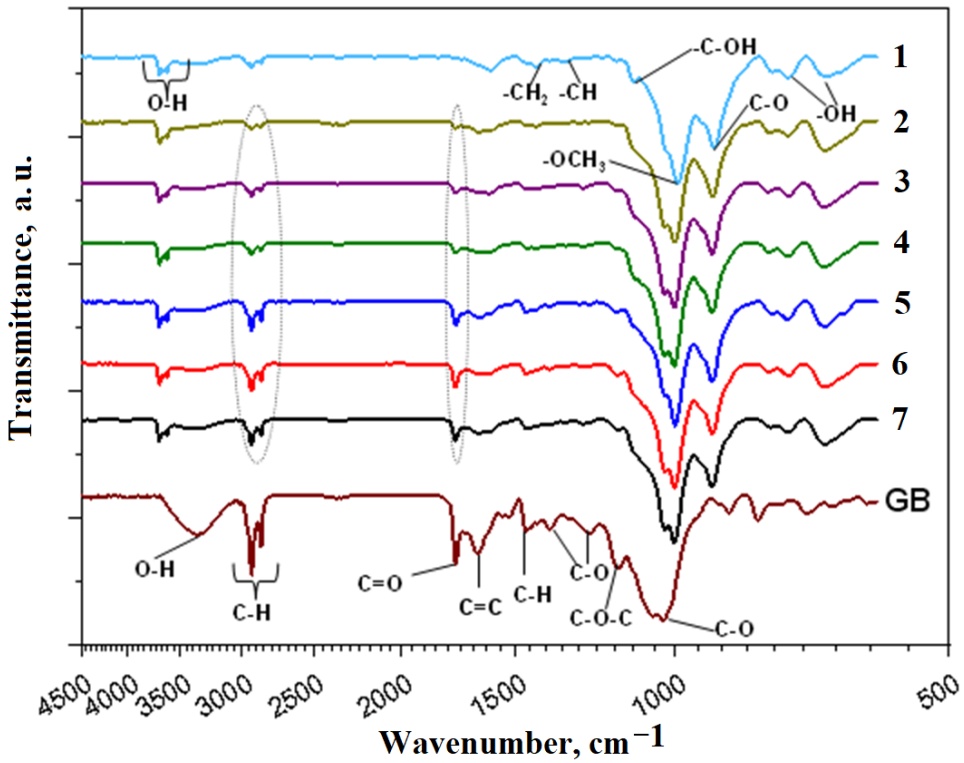


Figure 5. ATR-FTIR for composite materials, paper pulp, and Granbar (GB) SCGs.

The spectrum obtained for the paper-pulp-based material indicates the presence of adsorption bands at 1428, 1367, 1334, 1027, and 896 cm^{-1}, which can be attributed to the stretching and bending vibrations of the -CH_2, -CH, -C-OH, -OCH_3, and C-O bonds in cellulose [90]. Additionally, two peaks at 3680 and 3600 cm^{-1} are also identified in the spectra of the composite materials. These can be assigned to the lignin phenolic hydroxyl groups [91] and to the O-H stretches of water associated with the cellulose OH groups [92]. Moreover, the position of the O-H bands is dependent on the strength of the hydrogen bonds. Thus, O-H-O intramolecular H-bonds in cellulose yield absorptions at lower wavenumbers (3308 cm^{-1}), as evidenced in the IR spectrum of the SCGs [93]. These peaks have the same intensity for all composite materials and can be associated with the vibration of the O-H bond in the paper pulp.

The modification of the IR spectra in the O-H spectral region was better achieved via the calculation of H-bond distance (R) and energy (EH) since the presence of SCGs and binding water can affect the interchange ratio between the matrix and filler, leading to a well ordered network. For this purpose, the Sederholm equation [94] was used as follows:

$$\Delta\nu\ (cm^{-1}) = 4.43 \times 10^3 \times (2.84 - R) \quad (1)$$

where $\Delta\nu = \nu - \nu 0$, $\nu 0$ is the normal wavenumber corresponding to free O-H groups found at 3650 cm^{-1} and ν is the stretching wavenumber of the H-bonded O-H groups in the IR spectra of the analyzed samples.

The energy of the H bonds (E_H) was determined from the formulae [95]

$$E_H = \frac{1}{k}\frac{\nu_0 - \nu}{\nu_0} \quad (2)$$

where $\frac{1}{k}$ is a constant with the value of 2.625×10^2 kJ.

All the samples showed characteristic absorption of OH stretches connected by H bonding with water molecules (at about 3400 cm^{-1}) and SCG filler (at about 3300 cm^{-1}). Based on the position of these bands, the H-bond distances and energies were estimated and tabulated in Table 6.

Table 6. Spectral characteristics of OH region, H-bond energy, and distance for analyzed samples.

Sample	$\Delta\nu$ (cm^{-1})		E_H (kJ/mol)		R (Å)		X_{IR} (%)
	$\Delta\nu_1$	$\Delta\nu_2$	E_H (Water Matrix)	E_H (SCG Matrix)	R (Water Matrix)	R (SCG Matrix)	A_{1370}/A_{2926} / A_{1430}/A_{910}
1	190	-	12.94	-	2.799	-	0.12/0.24
2	291	280	20.93	20.14	2.774	2.776	0.27/0.12
3	213	308	15.32	22.15	2.792	2.770	0.28/0.11
4	194	257	13.95	18.48	2.796	2.781	0.25/0.16
5	180	306	12.94	22.00	2.799	2.770	0.26/0.11
6	194	290	13.95	20.85	2.796	2.774	0.27/0.18
7	153	338	11.00	24.30	2.805	2.763	0.21/0.21
GC	342		24.59		2.763		

$\Delta\nu_1 = \nu_0 - \nu_{\text{water matrix}}$; $\Delta\nu_2 = \nu_0 - \nu_{\text{GC matrix}}$; X is crystallinity index.

One can observe that the concentration of bound water influences the intra- and intermolecular H bonding between the paper pulp and SCGs. The increase in the E_H characteristic for bound water demonstrates the perturbation of the structural order of the matrix. The decrease in the E_H specific to matrix–SCG interactions as compared with the E_H of SCGs also confirms the presence of intermolecular SCG–paper pulp interactions. The values of the E_H SCG matrix increased by adding high concentrations of SCGs (sample 7). The crystallinity index of the paper pulp calculated by ratios between the area corresponding to the OH groups and the area corresponding to the C-H groups (A_{1370}/A_{2926} and A_{1430}/A_{910}) also increased from 0.12 in sample 1 to 0.27–0.28 in samples 2–7, demonstrating an ordered organization of cellulose fibers within the networks [96].

The irradiation of the samples did not cause major changes (Figure 6) in the crystallinity of the consolidated matrix but only a decrease of 11% for the samples with lower SCG concentrations. At higher SCG concentrations, the crystallinity values are similar to those of the non-irradiated samples. The exposure of the composite materials to irradiation leads to the adsorption of energy by water molecules producing radicals (HO. and H.), which are further responsible for the generation of different radicals in the cellulose structure and the reorganization of molecular chains. Moreover, in the presence of oxygen, a peroxyl radical can be generated that can promote a marked degradation of the matrix with chain

disruption, ring opening, or stabilization by-products, which can also interact with SCG fillers, enhancing the stability of the networks [97].

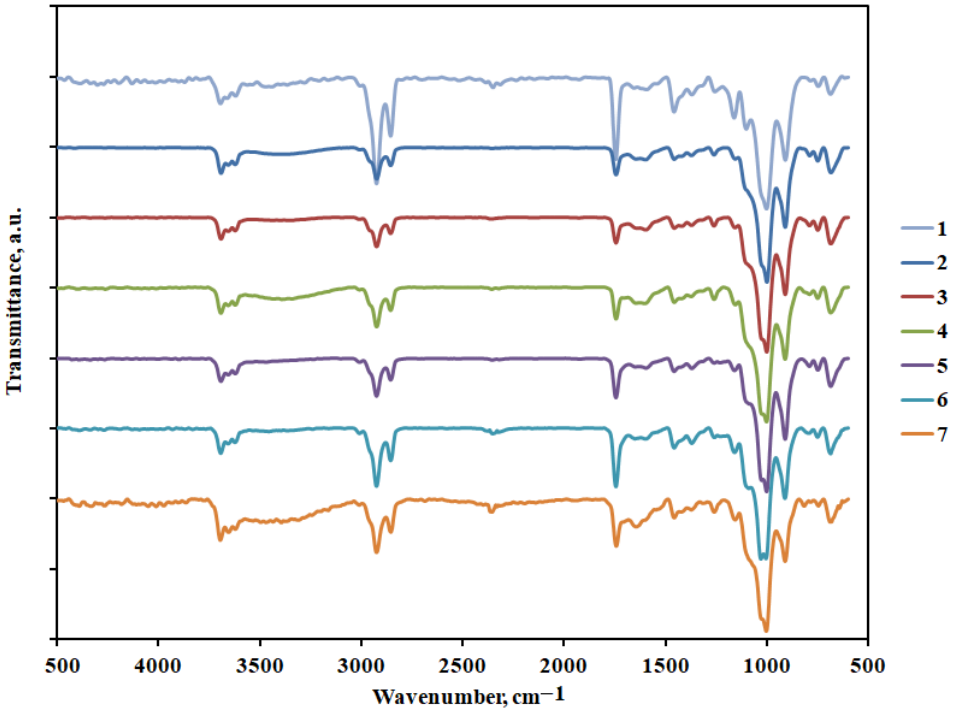


Figure 6. ATR-FTIR for composite materials after irradiation.

The analysis of the obtained results reveals that, for Granbar SCGs, there are peaks at 2923 cm^{-1}, 2853 cm^{-1}, and 1464 cm^{-1} specific to aliphatic C-H bonds, at 1743 cm^{-1} for characteristic C=O bands (esters), and at 1634 cm^{-1} for characteristic C=C bands (aromatic). The peaks at 1374 cm^{-1}, 1225 cm^{-1}, and 1026 cm^{-1} are characteristic C-O bands, while those at 1154 cm^{-1} are specific to C-O-C bonds, which can be attributed according to the literature to various monosaccharides and acid molecules, such as chlorogenic acid, caffeic acid, and coumaric acid [98,99]. The peak at 1634 cm^{-1} may also be associated with the presence of caffeine residues in the analyzed SCGs [100,101].

In the case of composite materials based on paper pulp and SCGs, the spectra presented in Figure 5 show an intensification of the peaks around 2850 and 2920 cm^{-1}, which are attributed to C-H bonds, as well as the peak around 1740 cm^{-1} corresponding to the carbonyl (C=O) bond vibration as the amount of SCGs in these samples increases from sample 2 to sample 7. These peaks have been attributed in the literature to the ester group of triglycerides found in lipids (fats) [100]. These results correlate with those obtained earlier via thermogravimetric analysis, where a peak appears at approximately 390 °C within the temperature range of 340–410 °C, and its intensity increases with the amount of SCGs in the composite materials, which has been associated with the degradation of the fats present in coffee residues.

In this study, the ATR-FTIR technique was effectively utilized to assess the primary functional groups within the structure of composite materials created from paper pulp and SCGs, as well as to gather information about their composition.

3.2.4. Rheological Characterization

An amplitude sweep is mainly performed to determine the linear viscoelastic (LVE) range of materials. The maximum strain up to which the value of the storage modulus G′ remains constant is called the limit strain and defines the limit of the LVE range. The value of the limit strain indicates the minimum amount of energy required to destabilize the material structure. This test provides valuable information regarding the mechanical and

structural stability of all the investigated samples [102]. The obtained results are presented in Figure 7.

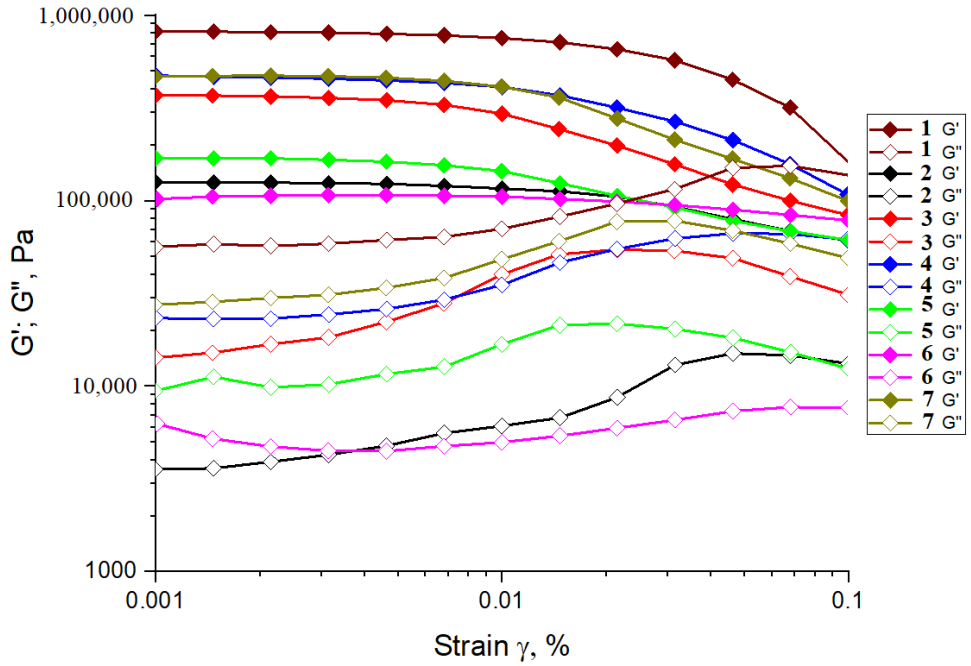


Figure 7. Amplitude sweep test for the analyzed samples.

The amplitude sweep indicated that the composites show weak strain behavior in the strain domain 0.001–0.1%. This finding indicates the formation of weak structural complexes, which cause retardation in the macromolecular chain dynamics of the cellulose from the paper pulp. All the composites exhibit a plateau in the low strain region, followed by a drop in the dynamic moduli. The decrease in the storage modulus value G′ is due to the dissociation of the entanglements and to the orientation of the chains along the strain direction. From the amplitude sweep curves (Figure 7), it is possible to note that the dynamic modulus value decreases with increasing SCG amount, exhibiting the same trend observed during the frequency sweep tests. The value of the limit strain decreases for the composites, indicating that the linear viscoelastic range is sensitive to the SCG content [103]. The value of the limit strain for the analyzed samples according to the data presented in Table 7 is between 0.005 and 0.01%.

Table 7. Rheological parameters of the analyzed samples.

Sample	γ, %	G′, MPa
1	0.01	0.814
2	0.01	0.126
3	0.005	0.368
4	0.005	0.472
5	0.005	0.170
6	0.01	0.102
7	0.005	0.466

The storage modulus of the composites increased from 0.102 MPa to 0.814 MPa depending on the SCG content. The inter-chain bonding of cellulose from paper pulp is more important than the strength of individual chains in determining the mechanical

stability of the material. Sample 1 (without SCGs) presents the highest value of the storage modulus [104].

The dynamic moduli are dependent on the interface between the cellulose and SCG particles. The contact area as well as the hydrogen bonds between the cellulose and SCG particles, together with the covalent bonds in the backbone of the cellulose chain, were found to be the controlling mechanical parameters that determine the mechanical stability of the composite materials [105].

In the LVE range, it is observed that G′>G″ for all the samples, thus indicating a solid-like behavior. The values obtained for the storage modulus G′ (Table 7) indicate that the analyzed samples show good resistance to strain. Sample 1 (100% paper pulp) shows the highest deformation resistance. Despite this, the samples containing SCGs with G′ values between 0.102 and 0.472 MPa can be considered as having sufficient deformation resistance for use in the preparation of seedling pots.

The frequency sweeps were performed at a constant amplitude of 0.005 or 0.01% (in the LVE range characteristic for each sample) over a frequency range between 0.1 and 100 rad/s.

In the frequency sweep diagrams, the storage modulus (G′) describes the elastic behavior of the sample, providing information about the stability and structural strength of the sample ("stiffness"), while the loss modulus (G″) provides information about the viscous behavior ("flexibility") [106]. High values of the storage modulus indicate the presence of a stable internal network of forces within the sample, a measure of its mechanical and structural stability.

The results obtained in the frequency sweep are shown in Figures 8 and 9. It was found that all the analyzed composites exhibit G′>G″. The storage modulus values are in the range of 0.1 to 1 MPa, and the complex viscosity lη*l ranges from 103 to 107 Pa*s. These results confirm that the analyzed samples exhibit good stability over time and good deformation resistance.

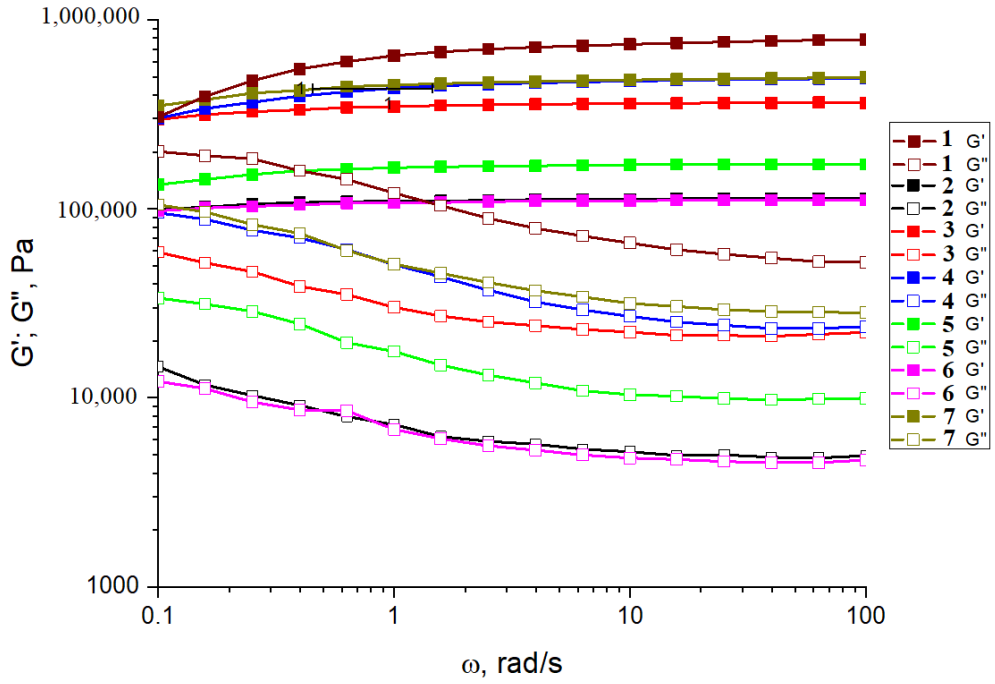


Figure 8. Frequency sweep test for the analyzed samples, dynamic moduli G′ and G″.

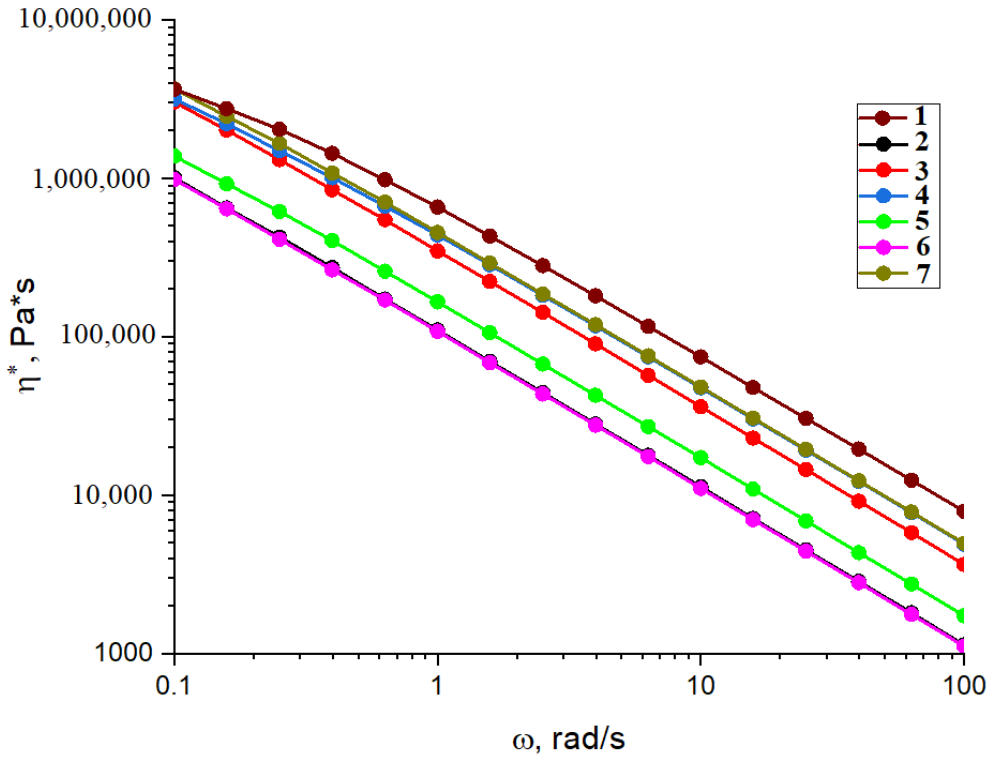


Figure 9. Frequency sweep test for the analyzed samples, complex viscosity lη*l.

The composite materials obtained in this study exhibit an excellent balance between low cost, sustainability, and good mechanical properties, making them ideal for temporary applications such as seedling pots. These materials incorporate a significantly higher amount of SCGs, with percentages ranging from 57% to 79%, in combination with paper pulp compared to other studies in the literature where the SCG values reach a maximum of 50% in composites with polymeric matrices such as PHBV [58], PBAT [59], or PLA [43]. The raw materials used to produce the composites in this study involve much lower production costs compared to other biodegradable alternatives (such as starch-based bioplastics or PLA) because they do not require complex industrial processes and are readily available. SCGs can be considered to be a waste material with no additional acquisition costs. Paper pulp can come from recycled paper or industrial residues, making it an economical and sustainable resource. Compared to PLA bioplastics or other polymer-based materials, however, this composite has lower moisture resistance and durability under intensive use conditions. The large-scale integration of SCGs into the composites developed in this study supports the circular economy by valorizing an organic waste that would otherwise end up in landfills, where it could generate methane emissions. Another major advantage of the composites produced in this study is that both SCGs and paper pulp are fully biodegradable, and the resulting composite decomposes quickly in the environment compared to alternatives such as PLA (which requires industrial composting conditions). After degradation, the composite material can act as a natural fertilizer due to the nitrogen and mineral content in the SCGs.

3.3. Challenges and Opportunities

Studies on the development of composite materials using paper pulp as the matrix, SCGs as the filler material, and water as the binding agent must continue in order to achieve materials with an optimal composition. These materials should combine the properties of the matrix—namely the paper pulp, which ensures the cohesion of the composite and the uniform distribution of filler particles—with those of the SCGs, which contribute to rigidity, texture, and the reduction in material density. To enhance the durability and strength of paper pulp and SCG-based composite materials, a natural binder, such as starch

or gelatin, could be included in the composition. Additionally, the research could focus on analyzing the presence of lignin in the SCGs within the paper pulp–SCG composites. Lignin may act as a plasticizer or even as a binding agent, thus contributing to the potential development of filaments for 3D printing. Lignin reduces the brittleness of the material and improves the cohesion between the cellulose fibers and SCGs. It interacts with other natural components, such as the hemicellulose and lipids in the SCGs, and imparts improved mechanical properties to the material. Moreover, lignin can contribute to achieving the malleability needed for extruding 3D printing filaments. The progress of such studies would be particularly important because the research available so far in the literature indicates the production of 3D printing filaments containing SCGs only in combination with PLA [43,107–110]. However, the widespread use of PLA in the production of 3D printing filaments raises the issue of waste disposal to minimize its environmental impact. Research has shown that, under natural conditions, in soil, the decomposition of PLA can take several years, and, in water, several decades [111,112].

4. Conclusions

The obtained results suggest that the mechanical properties of composites can be optimized through maximizing the formations of the contributing hydrogen bonds between cellulose from the paper pulp and SCG particles. The measurements revealed a solid-like behavior for the composites containing SCGs due to the formation of a cellulose–particle network that restricts the dynamics of cellulose chains. It was found that the inter-chain bonding strength plays a dominant role in the mechanical stability.

The composite materials derived from paper pulp and SCGs have been shown to be effective for manufacturing seedling pots, as evidenced by their characterization.

The seedling pots created in this study are produced at a low cost, are eco-friendly, exhibit thermal stability, show good long-term stability, and possess strong resistance to deformation.

Composite materials based on paper pulp and SCGs, following further processing and filament production, have the potential to be utilized in the fabrication of design objects through 3D printing.

Author Contributions: Conceptualization, G.L.; Methodology, G.L. and M.D.; Formal analysis, V.B., M.D., A.-M.I., M.-F.Z. and D.R.; Data curation, V.B. and M.D.; Visualization, V.B., M.D. and G.L.; Investigation, V.B., M.D., A.-M.I., M.-F.Z., D.R. and G.L.; Validation, M.D. and G.L.; Resources, M.D., M.-F.Z. and D.R.; Writing—original draft preparation, V.B., M.D., A.-M.I., M.-F.Z., D.R. and G.L.; Writing—review and editing, G.L. and M.D.; Supervision, G.L. All authors have read and agreed to the published version of the manuscript.

Funding: This research received no external funding.

Data Availability Statement: The original contributions presented in the study are included in the article; further inquiries can be directed to the corresponding authors.

Conflicts of Interest: The authors declare no conflicts of interest.

References

1. *Coffee Report and Outlook*; International Coffee Organization (ICO): London, UK, 2023; pp. 1–39.
2. *BEYOND COFFEE. Towards a Circular Coffee Economy*; International Coffee Organization (ICO): London, UK, 2023.
3. Yang, W.; Chang, W.; Zhang, J.; Yeoh, G.H.; Boyer, C.; Wang, C.H. Effects of waste coffee grounds on the mechanical properties, flame retardancy and toxic gas production of epoxy composites. *Mater. Des.* **2022**, *224*, 111347. [CrossRef]
4. Campos-Vega, R.; Loarca-Piña, G.; Vergara-Castañeda, H.A.; Oomah, B.D. Spent coffee grounds: A review on current research and future prospects. *Trends Food Sci. Technol.* **2015**, *45*, 24–36. [CrossRef]
5. Jin Cho, E.; Gyo Lee, Y.; Song, Y.; Nguyen, D.-T.; Bae, H.-J. An integrated process for conversion of spent coffee grounds into value-added materials. *Bioresour. Technol.* **2022**, *346*, 126618. [CrossRef] [PubMed]
6. Pacioni, T.R.; Soares, D.; Di Domenico, M.; Rosa, M.F.; Moreira, R.D.F.P.M.; José, H.J. Bio-syngas production from agro-industrial biomass residues by steam gasification. *Waste Manag.* **2016**, *58*, 221–229. [CrossRef]

7. Kourmentza, C.; Economou, C.N.; Tsafrakidou, P.; Kornaros, M. Spent coffee grounds make much more than waste: Exploring recent advances and future exploitation strategies for the valorization of an emerging food waste stream. *J. Clean. Prod.* **2018**, *172*, 980–992. [CrossRef]
8. Jang, H.; Ocon, J.D.; Lee, S.; Lee, J.K.; Lee, J. Direct power generation from waste coffee grounds in a biomass fuel cell. *J. Power Sources* **2015**, *296*, 433–439. [CrossRef]
9. Al-Hamamre, Z.; Foerster, S.; Hartmann, F.; Kröger, M.; Kaltschmitt, M. Oil extracted from spent coffee grounds as a renewable source for fatty acid methyl ester manufacturing. *Fuel* **2012**, *96*, 70–76. [CrossRef]
10. Caetano, N.S.; Caldeira, D.; Martins, A.A.; Mata, T.M. Valorisation of Spent Coffee Grounds: Production of Biodiesel via Enzymatic Catalysis with Ethanol and a Co-solvent. *Waste Biomass Valorization* **2017**, *8*, 1981–1994. [CrossRef]
11. Kondamudi, N.; Mohapatra, S.K.; Misra, M. Spent Coffee Grounds as a Versatile Source of Green Energy. *J. Agric. Food Chem.* **2008**, *56*, 11757–11760. [CrossRef]
12. Park, J.; Kim, B.; Lee, J.W. In-situ transesterification of wet spent coffee grounds for sustainable biodiesel production. *Bioresour. Technol.* **2016**, *221*, 55–60. [CrossRef]
13. Vardon, D.R.; Moser, B.R.; Zheng, W.; Witkin, K.; Evangelista, R.L.; Strathmann, T.J.; Rajagopalan, K.; Sharma, B.K. Complete Utilization of Spent Coffee Grounds To Produce Biodiesel, Bio-Oil, and Biochar. *ACS Sustain. Chem. Eng.* **2013**, *1*, 1286–1294. [CrossRef]
14. Wei, F.; Furihata, K.; Koda, M.; Hu, F.; Miyakawa, T.; Tanokura, M. Roasting Process of Coffee Beans as Studied by Nuclear Magnetic Resonance: Time Course of Changes in Composition. *J. Agric. Food Chem.* **2012**, *60*, 1005–1012. [CrossRef] [PubMed]
15. Castro, C.S.; Abreu, A.L.; Silva, C.L.T.; Guerreiro, M.C. Phenol adsorption by activated carbon produced from spent coffee grounds. *Water Sci. Technol.* **2011**, *64*, 2059–2065. [CrossRef] [PubMed]
16. Kim, M.-S.; Min, H.-G.; Koo, N.; Park, J.; Lee, S.-H.; Bak, G.-I.; Kim, J.-G. The effectiveness of spent coffee grounds and its biochar on the amelioration of heavy metals-contaminated water and soil using chemical and biological assessments. *J. Environ. Manag.* **2014**, *146*, 124–130. [CrossRef]
17. Kyzas, G.Z. Commercial Coffee Wastes as Materials for Adsorption of Heavy Metals from Aqueous Solutions. *Materials* **2012**, *5*, 1826–1840. [CrossRef]
18. Dávila-Guzmán, N.E.; de Jesús Cerino-Córdova, F.; Soto-Regalado, E.; Rangel-Mendez, J.R.; Díaz-Flores, P.E.; Garza-Gonzalez, M.T.; Loredo-Medrano, J.A. Copper Biosorption by Spent Coffee Ground: Equilibrium, Kinetics, and Mechanism. *CLEAN Soil Air Water* **2013**, *41*, 557–564. [CrossRef]
19. Davila-Guzman, N.E.; Cerino-Córdova, F.J.; Loredo-Cancino, M.; Rangel-Mendez, J.R.; Gómez-González, R.; Soto-Regalado, E. Studies of Adsorption of Heavy Metals onto Spent Coffee Ground: Equilibrium, Regeneration, and Dynamic Performance in a Fixed-Bed Column. *Int. J. Chem. Eng.* **2016**, *2016*, 9413879. [CrossRef]
20. Mantonanaki, A.; Pellera, F.M.; Gidarakos, E. Use of biochar generated from spent coffee grounds for the removal of Zn (II) from aqueous solutions. In Proceedings of the International Conference on Environmental Science and Technology, Rhodes, Greece, 3–5 September 2015; pp. 3–5.
21. Aouay, F.; Attia, A.; Dammak, L.; Ben Amar, R.; Deratani, A. Activated Carbon Prepared from Waste Coffee Grounds: Characterization and Adsorption Properties of Dyes. *Materials* **2024**, *17*, 3078. [CrossRef]
22. Oliveira, G.A.; Gevaerd, A.; Mangrich, A.S.; Marcolino-Junior, L.H.; Bergamini, M.F. Biochar obtained from spent coffee grounds: Evaluation of adsorption properties and its application in a voltammetric sensor for lead (II) ions. *Microchem. J.* **2021**, *165*, 106114. [CrossRef]
23. Jeníček, L.; Tunklová, B.; Malaťák, J.; Neškudla, M.; Velebil, J. Use of Spent Coffee Ground as an Alternative Fuel and Possible Soil Amendment. *Materials* **2022**, *15*, 6722. [CrossRef]
24. Zungu, V.; Hadebe, L.; Mpungose, P.; Hamza, I.; Amaku, J.; Gumbi, B. Fabrication of Biochar Materials from Biowaste Coffee Grounds and Assessment of Its Adsorbent Efficiency for Remediation of Water-Soluble Pharmaceuticals. *Sustainability* **2022**, *14*, 2931. [CrossRef]
25. de Souza, L.Z.M.; Pinto, B.C.; Alves, A.B.; de Oliveira Ribeiro, A.V.; Teodoro Feliciano, D.C.; da Silva, L.H.; Moraes Dias, T.T.; Yılmaz, M.; de Oliveira, M.A.; da Silva Bezerra, A.C.; et al. Ecotoxicological Effects of Biochar Obtained from Spent Coffee Grounds. *Mater. Res.* **2022**, *25*, e20220013. [CrossRef]
26. Andrade, T.S.; Vakros, J.; Mantzavinos, D.; Lianos, P. Biochar obtained by carbonization of spent coffee grounds and its application in the construction of an energy storage device. *Chem. Eng. J. Adv.* **2020**, *4*, 100061. [CrossRef]
27. Liu, S.-H.; Huang, Y.-Y. Valorization of coffee grounds to biochar-derived adsorbents for CO_2 adsorption. *J. Clean. Prod.* **2018**, *175*, 354–360. [CrossRef]
28. Stylianou, M.; Christou, A.; Dalias, P.; Polycarpou, P.; Michael, C.; Agapiou, A.; Papanastasiou, P.; Fatta-Kassinos, D. Physicochemical and structural characterization of biochar derived from the pyrolysis of biosolids, cattle manure and spent coffee grounds. *J. Energy Inst.* **2020**, *93*, 2063–2073. [CrossRef]
29. Shin, J.; Lee, S.-H.; Kim, S.; Ochir, D.; Park, Y.; Kim, J.; Lee, Y.-G.; Chon, K. Effects of physicochemical properties of biochar derived from spent coffee grounds and commercial activated carbon on adsorption behavior and mechanisms of strontium ions (Sr^{2+}). *Environ. Sci. Pollut. Res.* **2021**, *28*, 40623–40632. [CrossRef]
30. Venkatesan, S.; Baloch, H.A.; Jamro, I.A.; Rafique, N. Evaluation of the production of hydrochar from spent coffee grounds under different operating conditions. *J. Water Process Eng.* **2022**, *49*, 103037. [CrossRef]

31. Cervera-Mata, A.; Lara, L.; Fernández-Arteaga, A.; Ángel Rufián-Henares, J.; Delgado, G. Washed hydrochar from spent coffee grounds: A second generation of coffee residues. Evaluation as organic amendment. *Waste Manag.* **2021**, *120*, 322–329. [CrossRef]
32. Hu, Y.; Gallant, R.; Salaudeen, S.; Farooque, A.A.; He, S. Hydrothermal Carbonization of Spent Coffee Grounds for Producing Solid Fuel. *Sustainability* **2022**, *14*, 8818. [CrossRef]
33. Tang, J.; Chen, Y.; He, L.; Li, Y.; Li, H.; Sun, F.; Liu, Y. Effect of hydrochar from sludge mixed with coffee grounds on the immobilization of Cu, Cr and Ni in soil. *Environ. Technol.* **2024**, 1–13. [CrossRef]
34. Dang, C.H.; Farru, G.; Glaser, C.; Fischer, M.G.; Libra, J.A. Enhancing the Fuel Properties of Spent Coffee Grounds through Hydrothermal Carbonization: Output Prediction and Post-Treatment Approaches. *Sustainability* **2024**, *16*, 338. [CrossRef]
35. Mukherjee, A.; Saha, B.; Niu, C.; Dalai, A.K. Preparation of activated carbon from spent coffee grounds and functionalization by deep eutectic solvent: Effect of textural properties and surface chemistry on CO2 capture performance. *J. Environ. Chem. Eng.* **2022**, *10*, 108815. [CrossRef]
36. Figueroa Campos, G.A.; Perez, J.P.H.; Block, I.; Sagu, S.T.; Saravia Celis, P.; Taubert, A.; Rawel, H.M. Preparation of Activated Carbons from Spent Coffee Grounds and Coffee Parchment and Assessment of Their Adsorbent Efficiency. *Processes* **2021**, *9*, 1396. [CrossRef]
37. Biegun, M.; Dymerska, A.; Chen, X.; Mijowska, E. Study of the Active Carbon from Used Coffee Grounds as the Active Material for a High-Temperature Stable Supercapacitor with Ionic-Liquid Electrolyte. *Materials* **2020**, *13*, 3919. [CrossRef]
38. Kusuma, J.; Indartono, Y.S.; Mujahidin, D. Biodiesel and activated carbon from arabica spent coffee grounds. *MethodsX* **2023**, *10*, 102185. [CrossRef]
39. Ren, J.; Chen, N.; Wan, L.; Li, G.; Chen, T.; Yang, F.; Sun, S. Preparation of High-Performance Activated Carbon from Coffee Grounds after Extraction of Bio-Oil. *Molecules* **2021**, *26*, 257. [CrossRef]
40. Bartczak, P.; Stachowiak, J.; Szmitko, M.; Grząbka-Zasadzińska, A.; Borysiak, S. Multifunctional Polyurethane Composites with Coffee Grounds and Wood Sawdust. *Materials* **2023**, *16*, 278. [CrossRef]
41. Yoo, J.; Chang, S.J.; Wi, S.; Kim, S. Spent coffee grounds as supporting materials to produce bio-composite PCM with natural waxes. *Chemosphere* **2019**, *235*, 626–635. [CrossRef]
42. Leow, Y.; Yew, P.Y.M.; Chee, P.L.; Loh, X.J.; Kai, D. Recycling of spent coffee grounds for useful extracts and green composites. *RSC Adv.* **2021**, *11*, 2682–2692. [CrossRef]
43. Yu, W.; Yuan, T.; Yao, Y.; Deng, Y.; Wang, X. PLA/Coffee Grounds Composite for 3D Printing and Its Properties. *Forests* **2023**, *14*, 367. [CrossRef]
44. Masssijaya, S.Y.; Lubis, M.A.R.; Nissa, R.C.; Nurhamiyah, Y.; Nugroho, P.; Antov, P.; Lee, S.-H.; Papadopoulos, A.N.; Kusumah, S.S.; Karlinasari, L. Utilization of Spent Coffee Grounds as a Sustainable Resource for the Synthesis of Bioplastic Composites with Polylactic Acid, Starch, and Sucrose. *J. Compos. Sci.* **2023**, *7*, 512. [CrossRef]
45. Hunsub, P.; Ngamprasertsith, S.; Prichapan, N.; Sakdasri, W.; Karnchanatat, A.; Sawangkeaw, R. Production of Protein Hydrolysates from Spent Coffee Grounds via Microwave, Enzymatic, and Subcritical Water Extractions and Their Combination. *Biol. Life Sci. Forum* **2023**, *26*, 43. [CrossRef]
46. Burniol-Figols, A.; Cenian, K.; Skiadas, I.V.; Gavala, H.N. Integration of chlorogenic acid recovery and bioethanol production from spent coffee grounds. *Biochem. Eng. J.* **2016**, *116*, 54–64. [CrossRef]
47. Mussatto, S.I.; Machado, E.M.S.; Carneiro, L.M.; Teixeira, J.A. Sugars metabolism and ethanol production by different yeast strains from coffee industry wastes hydrolysates. *Appl. Energy* **2012**, *92*, 763–768. [CrossRef]
48. Cruz, M.V.; Paiva, A.; Lisboa, P.; Freitas, F.; Alves, V.D.; Simões, P.; Barreiros, S.; Reis, M.A.M. Production of polyhydroxyalkanoates from spent coffee grounds oil obtained by supercritical fluid extraction technology. *Bioresour. Technol.* **2014**, *157*, 360–363. [CrossRef] [PubMed]
49. Battista, F.; Fino, D.; Mancini, G. Optimization of biogas production from coffee production waste. *Bioresour. Technol.* **2016**, *200*, 884–890. [CrossRef]
50. Kim, J.; Kim, H.; Baek, G.; Lee, C. Anaerobic co-digestion of spent coffee grounds with different waste feedstocks for biogas production. *Waste Manag.* **2017**, *60*, 322–328. [CrossRef]
51. Valero, D.; Montes, J.A.; Rico, J.L.; Rico, C. Influence of headspace pressure on methane production in Biochemical Methane Potential (BMP) tests. *Waste Manag.* **2016**, *48*, 193–198. [CrossRef]
52. Qiao, W.; Takayanagi, K.; Shofie, M.; Niu, Q.; Yu, H.Q.; Li, Y.-Y. Thermophilic anaerobic digestion of coffee grounds with and without waste activated sludge as co-substrate using a submerged AnMBR: System amendments and membrane performance. *Bioresour. Technol.* **2013**, *150*, 249–258. [CrossRef]
53. Vítěz, T.; Koutný, T.; Šotnar, M.; Chovanec, J. On the spent coffee grounds biogas production. *Acta Univ. Agric. Silvic. Mendel. Brun.* **2016**, *64*, 1279–1282. [CrossRef]
54. Neves, L.; Oliveira, R.; Alves, M.M. Anaerobic co-digestion of coffee waste and sewage sludge. *Waste Manag.* **2006**, *26*, 176–181. [CrossRef] [PubMed]
55. Abouelenien, F.; Namba, Y.; Kosseva, M.R.; Nishio, N.; Nakashimada, Y. Enhancement of methane production from co-digestion of chicken manure with agricultural wastes. *Bioresour. Technol.* **2014**, *159*, 80–87. [CrossRef]

56. Nguyen, T.A.; Oanh, D.T.Y.; Ngo, T.V.; Nguyen, T.H.; Nguyen, T.T.P.; Bui, T.T.T.; Dam, X.T.; Nguyen, K.A.; Nguyen, M.V.; Nguyen, Q.T. Transforming environmental sustainability: Lime-treated used coffee grounds for innovative eco-friendly epoxy composite materials. *Vietnam J. Chem.* **2024**, *1*, 1–15. [CrossRef]
57. de Bomfim, A.S.C.; de Oliveira, D.M.; Voorwald, H.J.C.; de Carvalho Benini, K.C.C.; Dumont, M.-J.; Rodrigue, D. Valorization of Spent Coffee Grounds as Precursors for Biopolymers and Composite Production. *Polymers* **2022**, *14*, 437. [CrossRef] [PubMed]
58. Alharbi, M.; Bairwan, R.D.; Rizg, W.Y.; Khalil, H.P.S.A.; Murshid, S.S.A.; Sindi, A.M.; Alissa, M.; Saharudin, N.I.; Abdullah, C.K. Enhancement of spent coffee grounds as biofiller in biodegradable polymer composite for sustainable packaging. *Polym. Compos.* **2024**, *45*, 9317–9334. [CrossRef]
59. Moustafa, H.; Guizani, C.; Dufresne, A. Sustainable biodegradable coffee grounds filler and its effect on the hydrophobicity, mechanical and thermal properties of biodegradable PBAT composites. *J. Appl. Polym. Sci.* **2017**, *134*, 44498. [CrossRef]
60. Cataldo, V.A.; Cavallaro, G.; Lazzara, G.; Milioto, S.; Parisi, F. Coffee grounds as filler for pectin: Green composites with competitive performances dependent on the UV irradiation. *Carbohydr. Polym.* **2017**, *170*, 198–205. [CrossRef]
61. Lee, H.K.; Park, Y.G.; Jeong, T.; Song, Y.S. Green nanocomposites filled with spent coffee grounds. *J. Appl. Polym. Sci.* **2015**, *132*, 2–7. [CrossRef]
62. de Bomfim, A.S.C.; de Oliveira, D.M.; de Carvalho Benini, K.C.C.; Cioffi, M.O.H.; Voorwald, H.J.C.; Rodrigue, D. Effect of Spent Coffee Grounds on the Crystallinity and Viscoelastic Behavior of Polylactic Acid Composites. *Polymers* **2023**, *15*, 2719. [CrossRef]
63. Jaramillo, L.Y.; Vásquez-Rendón, M.; Upegui, S.; Posada, J.C.; Romero-Sáez, M. Polyethylene-coffee husk eco-composites for production of value-added consumer products. *Sustain. Environ. Res.* **2021**, *31*, 34. [CrossRef]
64. Haile, A.; Gelebo, G.G.; Tesfaye, T.; Mengie, W.; Mebrate, M.A.; Abuhay, A.; Limeneh, D.Y. Pulp and paper mill wastes: Utilizations and prospects for high value-added biomaterials. *Bioresour. Bioprocess.* **2021**, *8*, 35. [CrossRef] [PubMed]
65. Semple, K.E.; Zhou, C.; Rojas, O.J.; Nkeuwa, W.N.; Dai, C. Moulded pulp fibers for disposable food packaging: A state-of-the-art review. *Food Packag. Shelf Life* **2022**, *33*, 100908. [CrossRef]
66. Singh, A.K.; Itkor, P.; Lee, M.; Shin, J.; Lee, Y.S. Promoting sustainable packaging applications in the circular economy by exploring and advancing molded pulp materials for food products: A review. *Crit. Rev. Food Sci. Nutr.* **2023**, *63*, 11010–11025. [CrossRef] [PubMed]
67. Tomadoni, B.; Merino, D.; Alvarez, V.A. Biodegradable Materials for Planting Pots. *Adv. Appl. Bio Degrad. Green Compos.* **2020**, *68*, 85–103. [CrossRef]
68. Debnath, M.; Sarder, R.; Pal, L.; Hubbe, M. Molded pulp packaging review. *Bioresources* **2022**, *17*, 3810–3870. [CrossRef]
69. Zhang, Y.; Duan, C.; Bokka, S.K.; He, Z.; Ni, Y. Molded fiber and pulp products as green and sustainable alternatives to plastics: A mini review. *J. Bioresour. Bioprod.* **2022**, *7*, 14–25. [CrossRef]
70. Didone, M.; Saxena, P.; Brilhuis-Meijer, E.; Tosello, G.; Bissacco, G.; Mcaloone, T.C.; Pigosso, D.C.A.; Howard, T.J. Moulded Pulp Manufacturing: Overview and Prospects for the Process Technology. *Packag. Technol. Sci.* **2017**, *30*, 231–249. [CrossRef]
71. Döhler, N.; Wellenreuther, C.; Wolf, A. Market dynamics of biodegradable bio-based plastics: Projections and linkages to European policies. *EFB Bioecon. J.* **2022**, *2*, 100028. [CrossRef]
72. Baek, B.S.; Park, J.W.; Lee, B.H.; Kim, H.J. Development and Application of Green Composites: Using Coffee Ground and Bamboo Flour. *J. Polym. Environ.* **2013**, *21*, 702–709. [CrossRef]
73. Chaplin, M.F. Fibre and water binding. *Proc. Nutr. Soc.* **2003**, *62*, 223–227. [CrossRef]
74. Bejenari, V.; Marcu, A.; Ipate, A.-M.; Rusu, D.; Tudorachi, N.; Anghel, I.; Şofran, I.-E.; Lisa, G. Physicochemical characterization and energy recovery of spent coffee grounds. *J. Mater. Res. Technol.* **2021**, *15*, 4437–4451. [CrossRef]
75. Bejenari, V.; Lisa, C.; Cernătescu, C.; Mămăligă, I.; Lisa, G. Isothermal Drying Kinetic Study of Spent Coffee Grounds Using Thermogravimetric Analysis. *Int. J. Chem. Eng.* **2022**, *2022*, 2312147. [CrossRef]
76. Lengowski, E.C.; de Muñiz, G.I.B.; de Andrade, A.S.; Simon, L.C.; Nisgoski, S. Morphological, physical and thermal characterization of microfibrillated cellulose. *Rev. Árvore* **2018**, *42*, e420113. [CrossRef]
77. Shawky Sol, A.; Sakran She, M.; Ahmad, F.; Abdel-Atty, M. Evaluation of Paper Pulp and Paper Making Characteristics Produced from Different African Woody Trees Grown in Egypt. *Res. J. For.* **2017**, *11*, 19–27. [CrossRef]
78. Małachowska, E.; Dubowik, M.; Lipkiewicz, A.; Przybysz, K.; Przybysz, P. Analysis of Cellulose Pulp Characteristics and Processing Parameters for Efficient Paper Production. *Sustainability* **2020**, *12*, 7219. [CrossRef]
79. Ballesteros, L.F.; Teixeira, J.A.; Mussatto, S.I. Chemical, Functional, and Structural Properties of Spent Coffee Grounds and Coffee Silverskin. *Food Bioprocess Technol.* **2014**, *7*, 3493–3503. [CrossRef]
80. Özmeral, N.; Işık, M.; Sogancioglu Kalem, M.; Ahmetli, G. Lignocellulose coffee waste-based epoxy composites: Effect of various treatment methods on composite properties. *Cellulose* **2023**, *30*, 3589–3609. [CrossRef]
81. Dang, C.-H.; Nguyen, T.-D. Physicochemical Characterization of Robusta Spent Coffee Ground Oil for Biodiesel Manufacturing. *Waste Biomass Valorization* **2019**, *10*, 2703–2712. [CrossRef]
82. Fermoso, J.; Mašek, O. Thermochemical decomposition of coffee ground residues by TG-MS: A kinetic study. *J. Anal. Appl. Pyrolysis* **2018**, *130*, 358–367. [CrossRef]
83. Chinga-Carrasco, G.; Miettinen, A.; Luengo Hendriks, C.L.; Kristofer, E.; Kataj, M. Structural Characterisation of Kraft Pulp Fibres and Their Nanofibrillated Materials for Biodegradable Composite Applications. In *Nanocomposites and Polymers with Analytical Methods*; BoD—Books on Demand: Norderstedt, Germany, 2011. [CrossRef]

84. Safarik, I.; Horska, K.; Svobodova, B.; Safarikova, M. Magnetically modified spent coffee grounds for dyes removal. *Eur. Food Res. Technol.* **2012**, *234*, 345–350. [CrossRef]
85. Le, V.T.; Pham, T.M.; Doan, V.D.; Lebedeva, O.E.; Nguyen, H.T. Removal of Pb(ii) ions from aqueous solution using a novel composite adsorbent of Fe3o4/PVA/spent coffee grounds. *Sep. Sci. Technol.* **2019**, *54*, 3070–3081. [CrossRef]
86. Hanafiah, S.F.M.; Danial, W.H.; Samah, M.A.A.; Samad, W.Z.; Susanti, D.; Salim, R.M.; Majid, Z.A. Extraction and characterization of microfibrillated and nanofibrillated cellulose from office paper waste. *Malays. J. Anal. Sci.* **2019**, *23*, 901–913. [CrossRef]
87. Cervera-Mata, A.; Pastoriza, S.; Rufián-Henares, J.Á.; Párraga, J.; Martín-García, J.M.; Delgado, G. Impact of spent coffee grounds as organic amendment on soil fertility and lettuce growth in two Mediterranean agricultural soils. *Arch. Agron. Soil Sci.* **2018**, *64*, 790–804. [CrossRef]
88. Ronga, D.; Parisi, M.; Barbieri, L.; Lancellotti, I.; Andreola, F.; Bignami, C. Valorization of Spent Coffee Grounds, Biochar and other residues to Produce Lightweight Clay Ceramic Aggregates Suitable for Nursery Grapevine Production. *Horticulturae* **2020**, *6*, 58. [CrossRef]
89. Andreola, F.; Borghi, A.; Pedrazzi, S.; Allesina, G.; Tartarini, P.; Lancellotti, I.; Barbieri, L. Spent Coffee Grounds in the Production of Lightweight Clay Ceramic Aggregates in View of Urban and Agricultural Sustainable Development. *Materials* **2019**, *12*, 3581. [CrossRef]
90. Hospodarova, V.; Singovszka, E.; Stevulova, N. Characterization of Cellulosic Fibers by FTIR Spectroscopy for Their Further Implementation to Building Materials. *Am. J. Anal. Chem.* **2018**, *09*, 303–310. [CrossRef]
91. Savy, D.; Mazzei, P.; Roque, R.; Nuzzo, A.; Bowra, S.; Santos, R. Structural recognition of lignin isolated from bioenergy crops by subcritical water: Ethanol extraction. *Fuel Process. Technol.* **2015**, *138*, 637–644. [CrossRef]
92. Olsson, A.-M.; Salmén, L. The association of water to cellulose and hemicellulose in paper examined by FTIR spectroscopy. *Carbohydr. Res.* **2004**, *339*, 813–818. [CrossRef]
93. Kesari, K.K.; Leppänen, M.; Ceccherini, S.; Seitsonen, J.; Väisänen, S.; Altgen, M.; Johansson, L.-S.; Maloney, T.; Ruokolainen, J.; Vuorinen, T. Chemical characterization and ultrastructure study of pulp fibers. *Mater. Today Chem.* **2020**, *17*, 100324. [CrossRef]
94. Pimentel, G.C.; Sederholm, C.H. Correlation of Infrared Stretching Frequencies and Hydrogen Bond Distances in Crystals. *J. Chem. Phys.* **1956**, *24*, 639–641. [CrossRef]
95. Struszczyk, H. Modification of Lignins. III. Reaction of Lignosulfonates with Chlorophosphazenes. *J. Macromol. Sci. Part A Chem.* **1986**, *23*, 973–992. [CrossRef]
96. Sdrobiş, A.; Cazacu, G.; Totolin, M.; Sdrobi, A. Alkaline solution swelling of fatty acids-modified softwood kraft pulp fibers. *Cellul. Chem. Technol.* **2011**, *45*, 329–338.
97. List, R.; Gonzalez-Lopez, L.; Ashfaq, A.; Zaouak, A.; Driscoll, M.; Al-Sheikhly, M. On the Mechanism of the Ionizing Radiation-Induced Degradation and Recycling of Cellulose. *Polymers* **2023**, *15*, 4483. [CrossRef]
98. Reis, N.; Franca, A.S.; Oliveira, L.S. Performance of diffuse reflectance infrared Fourier transform spectroscopy and chemometrics for detection of multiple adulterants in roasted and ground coffee. *LWT—Food Sci. Technol.* **2013**, *53*, 395–401. [CrossRef]
99. Auguścik-Królikowska, M.; Ryszkowska, J.; Ambroziak, A.; Szczepkowski, L.; Oliwa, R.; Oleksy, M. The structure and properties of viscoelastic polyurethane foams with fillers from coffee grounds. *Polimery* **2020**, *65*, 708–718. [CrossRef]
100. Zarrinbakhsh, N.; Wang, T.; Rodriguez-Uribe, A.; Misra, M.; Mohanty, A.K. Characterization of waste and coproducts from the coffee industry for composite material production. *BioResources* **2016**, *11*, 7637–7653. [CrossRef]
101. Ramos-Andrés, M.; Andrés-Iglesias, C.; García-Serna, J. Production of molecular weight fractionated hemicelluloses hydrolyzates from spent coffee grounds combining hydrothermal extraction and a multistep ultrafiltration/diafiltration. *Bioresour. Technol.* **2019**, *292*, 121940. [CrossRef]
102. Gafiţanu, C.A.; Filip, D.; Cernătescu, C.; Ibănescu, C.; Danu, M.; Pâslaru, E.; Rusu, D.; Tuchiluş, C.G.; Macocinschi, D. Formulation and evaluation of anise-based bioadhesive vaginal gels. *Biomed. Pharmacother.* **2016**, *83*, 485–495. [CrossRef] [PubMed]
103. Arrigo, R.; Jagdale, P.; Bartoli, M.; Tagliaferro, A.; Malucelli, G. Structure–Property Relationships in Polyethylene-Based Composites Filled with Biochar Derived from Waste Coffee Grounds. *Polymers* **2019**, *11*, 1336. [CrossRef]
104. Wang, Q.; Xiao, S.; Shi, S.Q. The effect of hemicellulose content on mechanical strength, thermal stability, and water resistance of cellulose-rich fiber material from poplar. *BioResources* **2019**, *14*, 5288–5300. [CrossRef]
105. Zhang, N.; Li, S.; Xiong, L.; Hong, Y.; Chen, Y. Cellulose-hemicellulose interaction in wood secondary cell-wall. *Model. Simul. Mater. Sci. Eng.* **2015**, *23*, 85010. [CrossRef]
106. Culeţu, A.; Mohan, G.; Duță, D.E. Rheological Characterization of the Dough with Added Dietary Fiber by Rheometer: A Review. *Bull. Univ. Agric. Sci. Vet. Med. Cluj-Napoca. Food Sci. Technol.* **2020**, *77*, 13–24. [CrossRef]
107. Boughanmi, O.; Allegue, L.; Marouani, H.; Koubaa, A. Experimental Investigations of the Influence of Spent Coffee Grounds Content on PLA Based Composite for 3D Printing. *Polym. Eng. Sci.* **2024**, *64*, 226–233. [CrossRef]
108. Boughanmi, O.; Allegue, L.; Marouani, H.; Koubaa, A.; Fouad, Y. Repetitive recycling effects on mechanical characteristics of poly-lactic acid and PLA/spent coffee grounds composite used for 3D printing filament. *Polym. Eng. Sci.* **2024**, *64*, 5613–5626. [CrossRef]
109. Paramatti, M.; Romani, A.; Pugliese, G.; Levi, M. PLA Feedstock Filled with Spent Coffee Grounds for New Product Applications with Large-Format Material Extrusion Additive Manufacturing. *ACS Omega* **2024**, *9*, 6423–6431. [CrossRef]

110. Li, S.; Shi, C.; Sun, S.; Chan, H.; Lu, H.; Nilghaz, A.; Tian, J.; Cao, R. From brown to colored: Polylactic acid composite with micro/nano-structured white spent coffee grounds for three-dimensional printing. *Int. J. Biol. Macromol.* **2021**, *174*, 300–308. [CrossRef]
111. Beltrán-Sanahuja, A.; Benito-Kaesbach, A.; Sánchez-García, N.; Sanz-Lázaro, C. Degradation of conventional and biobased plastics in soil under contrasting environmental conditions. *Sci. Total Environ.* **2021**, *787*, 147678. [CrossRef]
112. Royer, S.-J.; Greco, F.; Kogler, M.; Deheyn, D.D. Not so biodegradable: Polylactic acid and cellulose/plastic blend textiles lack fast biodegradation in marine waters. *PLoS ONE* **2023**, *18*, e0284681. [CrossRef]

Disclaimer/Publisher's Note: The statements, opinions and data contained in all publications are solely those of the individual author(s) and contributor(s) and not of MDPI and/or the editor(s). MDPI and/or the editor(s) disclaim responsibility for any injury to people or property resulting from any ideas, methods, instructions or products referred to in the content.